EARTH SURFACE PROCESSES AND LANDFORMS
Earth Surf. Process. Landforms **34**, 1726–1742 (2009)

Published online in Wiley InterScience
(www.interscience.wiley.com) DOI: 10.1002/esp.1856

Quantifying sediment storage in a high alpine valley (Turtmanntal, Switzerland)

Jan-Christoph Otto,[1]* Lothar Schrott,[1] Michel Jaboyedoff[2] and Richard Dikau[3]
[1] Department of Geography and Geology, University of Salzburg, Salzburg, Austria
[2] Institut de géomatique et d'analyse du risqué, Université de Lausanne, Lausanne, Switzerland
[3] Department of Geography, University of Bonn, Bonn, Germany

Received 8 September 2008; Revised 18 May 2009; Accepted 1 June 2009

*Correspondence to: Jan-Christoph Otto, Department of Geography and Geology, University of Salzburg, Hellbrunnerstrasse 34, 5020 Salzburg, Austria. E-mail: jan-christoph.otto@sbg.ac.at

ESPL
Earth Surface Processes and Landforms

ABSTRACT: The determination of sediment storage is a critical parameter in sediment budget analyses. But, in many sediment budget studies the quantification of magnitude and time-scale of sediment storage is still the weakest part and often relies on crude estimations only, especially in large drainage basins (>100 km²). We present a new approach to storage quantification in a meso-scale alpine catchment of the Swiss Alps (Turtmann Valley, 110 km²).

The quantification of depositional volumes was performed by combining geophysical surveys and geographic information system (GIS) modelling techniques. Mean thickness values of each landform type calculated from these data was used to estimate the sediment volume in the hanging valleys and the trough slopes. Sediment volume of the remaining subsystems was determined by modelling an assumed parabolic bedrock surface using digital elevation model (DEM) data.

A total sediment volume of $781{\cdot}3\times10^6$–$1005{\cdot}7\times10^6$ m³ is deposited in the Turtmann Valley. Over 60% of this volume is stored in the 13 hanging valleys. Moraine landforms contain over 60% of the deposits in the hanging valleys followed by sediment stored on slopes (20%) and rock glaciers (15%).

For the first time, a detailed quantification of different storage types was achieved in a catchment of this size. Sediment volumes have been used to calculate mean denudation rates for the different processes ranging from 0·1 to 2·6 mm/a based on a time span of 10 ka.

As the quantification approach includes a number of assumptions and various sources of error the values given represent the order of magnitude of sediment storage that has to be expected in a catchment of this size. Copyright © 2009 John Wiley & Sons, Ltd.

KEYWORDS: Sediment storage; sediment budget; landform analysis; sediment cascade; GIS modelling

Introduction

In mountain environments sediment fluxes are heavily influenced by topography and past and present glaciations. Accumulation, storage and release of sediment in mountain areas affected by glaciations operate on different spatial and temporal scales (Church and Ryder, 1972; Ballantyne, 2002). Process rates and operation times changed in the past generating a sequence of landforms that compose today's land surface. However, the response time to impacts of past glaciations on the landscape seems to be very variable leading to different models of paraglacial landscape response (Church and Slaymaker, 1989; Harbor and Warburton, 1993; Ballantyne, 2003; Dadson and Church, 2005). Depositional landforms are often assembled in a nested manner, creating neighbouring, overlapping, or underlying land surface patterns indicating coupling and decoupling relationships between landforms and the existence of a sediment cascade system structure (Caine, 1974). Ballantyne (2003) considers the determination of storage volume as a critical parameter for the construction of a paraglacial sediment budget. For most sediment budget studies the quantification of magnitude and time-scale of sediment storage is still the weakest part. At the same time, it is considered to be the most important link between sediment flux and landform evolution creating highly variable residence times and changing buffering capacities of sediment flux systems (Slaymaker and Spencer, 1998; Fryirs and Brierley, 2001). In alpine environments removal or remobilization of sediment from elevated locations, for example by debris flows or landslides, may constitute a hazard to life and infrastructure below, which comes increasingly into focus in relation to the observed climatic changes in many mountain areas (Zimmermann and Haeberli, 1992; Kääb and Reynolds, 2005). Especially melting of mountain permafrost in loose deposits affects the role of sediment storage causing a remobilization of material that has been stable for decades to thousands of years in upper catchment areas (Harris, 2005).

Various methods have been applied in order to estimate sediment volumes in alpine budgets since early studies of

Jäckli (1957) and Rapp (1960). Basic geomorphological methods like mapping, topographic survey or photo interpretation are frequently used in landform distribution analysis (Jäckli, 1957; Rapp, 1960; Jordan and Slaymaker, 1991; Watanabe *et al.*, 1998; Curry, 1999). However, volume quantification of sediments is often based on estimations only (Church and Slaymaker, 1989; Owens and Slaymaker, 1992; Shroder *et al.*, 1999; Taylor and Kite, 2006).

Presently, geophysical methods, high resolution digital terrain data and geographic information system (GIS) techniques open up new possibilities for the quantification of sediment volumes. With the availability of digital elevation models (DEMs), simple geometric forms are used to represent actual landform shapes and used to estimate landform volume. For example, a half-cone shape has been used to represent a talus cone landform (Shroder *et al.*, 1999; Campbell and Church, 2003; Cossart and Fort, 2008). Following geomorphometric approaches for glacial valley description (Graf, 1970), quadratic or power-law equations have been applied to cross-sections of glacial valleys in order to estimate valley fill deposits (Schrott and Adams, 2002; Schrott *et al.*, 2003). However, this method tends to overestimate sediment volumes compared to geophysical data and can only be used as an initial estimate of storage (Schrott *et al.*, 2003). A new approach to estimate sediment volumes based solely on DEM data is introduced by Jaboyedoff and Derron (2005). Their interactive routine, named Sloping Local Base Level (SLBL) is based on geometric assumptions about the glacial trough shape. Using this technique, they calculated a volume of 118 km^3 of sediment deposited in the upper Rhone Valley trough, which correlates well with the available geophysical information on sediment thickness (e.g. Finckh and Frei, 1991). However, this approach is restricted to glacial trough valley deposits and has not been applied successfully to other landforms.

Shallow geophysical survey techniques like seismic refraction, direct current (d.c.) resistivity or ground penetrating radar are increasingly used to determine sediment volumes in alpine environments (Hoffmann and Schrott, 2002, Schrott and Adams, 2002). Facilitated by new light-weight equipment, new data processing tools and increasing computational power, geophysical techniques enable a fast, non-destructive and relatively low cost source of subsurface data especially in rugged, alpine terrain (Schrott and Sass, 2008). However, many studies using geophysics for sediment deposit quantification have often been restricted to single landforms and/or small catchments (<40 km^2), or very large valley fill deposits (e.g. Hinderer, 2001).

Thus, there is a lack of studies and quantification approaches in meso-scale catchments in alpine environments (>50 km^2 to <1000 km^2). In order to close this gap, this study investigates the relationship between landform distribution, storage volume and landform evolution in the Turtmann Valley (110 km^2) in the southern Swiss Alps (Figure 1).

Fundamental research questions of this study include:

- What is the distribution structure of depositional landforms in the Turtmann Valley?
- How much sediment is stored in the Turtmann valley?
- What does the distribution of depositional landforms and sediment volumes reveal about the post-glacial landform evolution of the valley?

This study, for the first time quantifies sediment deposits of different high alpine landforms in a meso-scale catchment by applying a combination of geophysical surveying and GIS modelling techniques at different scales.

Characteristics of the Study Area

The Turtmann Valley is a high alpine catchment located in the southern Swiss Alps between the Matter Valley and the Anniviers Valley (Figure 1A). The main stream of the valley, a tributary to the river Rhone, drains a 110 km^2 (139 km^2 real surface) catchment at altitudes between 620 m and 4200 m above sea level (a.s.l.) that is about 20 km long and up to 7 km wide. The Turtmann Valley is composed of a glacial trough surmounted by 14 hanging valleys to both sides. Ground levels of the hanging valleys increase from 2300 m to 2600 m a.s.l. towards the south. The hanging valleys contain a complex pattern of high alpine landforms including more than 80 recent and relict rock glaciers (Otto and Dikau, 2004; Nyenhuis, 2006). In addition to few small remains in the hanging valleys, two larger glaciers, the Turtmann and Brunegg Glaciers, at the valley head cover approximately 14% of the valley surface (Figure 1C). Lithology is mainly composed of Palaeozoic schist and gneiss with few locations of Mesozoic dolomite, limestone, and marble of the Penninic nappe Siviez-Mischabel (Bearth, 1978). Dry, continental climatic conditions result from the inner alpine location of the valley with a mean annual air temperature between 8·5 °C in the Rhone Valley (Sion) and 3·8 °C at 1825 m (Evolène, Anniviers Valley). Mean annual precipitation is about 500–600 mm (surrounding stations, data from www.meteoswiss.ch).

With respect to the sediment flux in this catchment, the valley can be subdivided into four subsystems: (i) hanging valleys, (ii) glacier forefield, (iii) main valley slopes, and (iv) main valley floor (Figure 1B). These subsystems form the superordinate sediment cascade structure, each containing a composition of lower level cascades composed of single landforms. The forefield of the Turtmann glacier terminates at an artificial dam that separates this subsystem from the main valley floor. The main valley slopes include all areas between the hanging valley and the trough floor (main valley floor) as well as the remaining slopes, which are not part of the hanging valleys.

Methods

The quantification of sediment storage combines different methods adapted to the four sedimentary subsystems of the valley (Table I). The level of detail and accuracy of the methods applied decrease with increasing scales of investigation. Some of the methods used rely on a number of assumptions that introduce uncertainties to the quantified volumes. These assumptions were necessary to cope with the large area under investigation. We will discuss the sources of errors towards the end of the paper. The most accurate sediment thickness data was produced by geophysical investigations on single landforms in one hanging valley. For all hanging valleys, sediment volumes have been calculated for each storage landform observed. In the other subsystems, the glacier forefield, the main trough and the trough slopes, the entire volume was determined without differentiation of different landform types within. Finally, a total sediment volume was calculated for the Turtmann Valley. These methods will be discussed here in more detail. The digital data used includes DEM (1 m resolution) and aerial photograph data (0·5 m resolution) produced by the HRSC (high resolution stereo camera) system (Otto *et al.*, 2007).

Storage quantification in the hanging valleys subsystem

To quantify the sediment stored in the hanging valleys, depositional landforms have been mapped in detail (Step 1, Table

DOI: 10.1002/esp

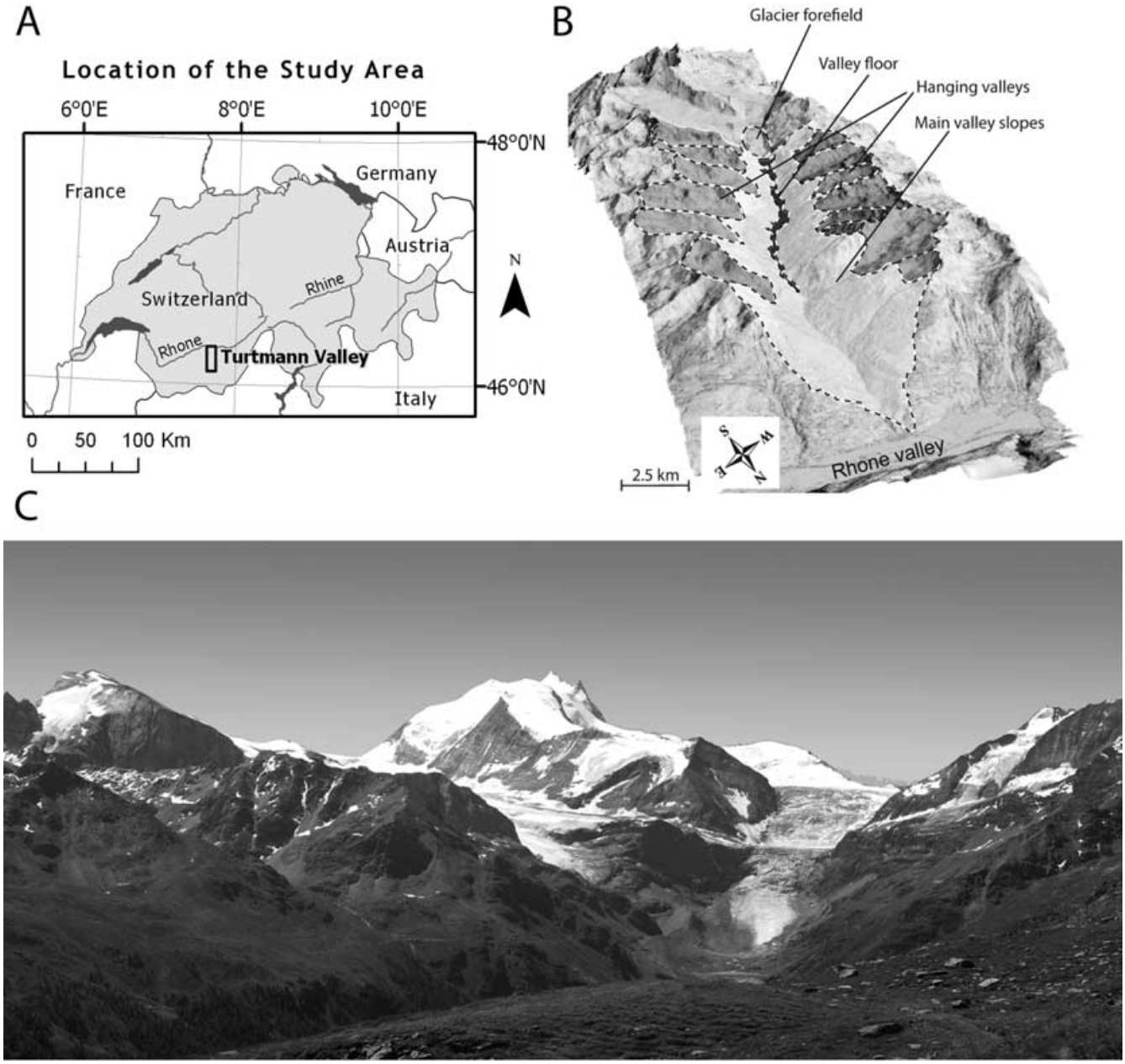

Figure 1. (A) Location of the Turtmann Valley, (B) sediment flux subsystems and (C) view towards south of the valley head showing the Turtmann glacier and some hanging valleys on the left of the picture.

I). Landform types include: talus slopes, talus cones, block slopes, moraine deposits, rock glaciers, rock fall deposits and alluvial deposits. Block slopes are straight debris covered slopes without adjacent rock walls. Moraine deposits include all types of glacial depositional landforms. Rock glaciers have been differentiated according to their activity (active, inactive, relict) in order to consider an assumed ice content in the calculations. Debris flow deposits are not frequently encountered in the hanging valleys and thus not considered in this study. A detailed description of the landform database can be found in Otto (2006).

In one hanging valley, the Hungerlitaelli, seismic refraction, d.c. resistivity and ground penetrating radar were applied at more than 35 profile locations to detect the debris-bedrock boundary (Step 2, Table I). Geophysical techniques measure specific physical properties of the subsurface, namely p-wave velocity (seismic refraction), electrical conductivity (d.c. resistivity) and electromagnetic wave velocity (ground penetrating radar) (Schrott and Sass, 2008). By interpreting the measured differences in physical properties, the debris–bedrock boundary can be located. Previous studies revealed that a combination of at least two of these techniques at each location increase the reliability of the results (Otto and Sass, 2006).

Sediment thickness data derived from geophysics was used to interpolate parabolic transects that should resemble the bedrock topography shaped by glacial abrasion [following the ideas of Harbor and Wheeler (1992)]. Due to the limited number of geophysical surveys the density of interpolation points was increased by adding points of assumed sediment thickness, for example near bedrock outcrops or by using landform height as minimum debris thickness. From these transects, a continuous bedrock surface was calculated (Step 3, Table I) and the mean sediment thickness was determined for the mapped landforms in this hanging valley (Step 4, Table I).

In order to consider the overlap of rock glacier deposits with glacial deposits in the central part of the hanging valley, two different methods of sediment thickness estimation have been

DOI: 10.1002/esp

Table I. Workflow and overview of methods applied for the storage quantification

Subsystem/scale	Workflow	Methods
 Single landforms	1. Mapping of storage landforms (hanging valleys)	Geomorphological mapping: - field work - photo interpretation - digital terrain analysis
	2. Determination of debris-bedrock surface (single landforms)	Geophysical sounding: - Refractions seismics - Electric resistivity tomography - Ground penetrating radar
 Single hanging valley (Hungerlitaelli)	3. Modelling of sediment thickness (single hanging valley)	Interpolation of bedrock depths: - Construction of parabolic profiles using geophysical data
	4. Calculation of mean sediment thickness of individual landforms (single hanging valley)	Deducting surface topography with bedrock topography; derive mean thickness per landform polygon: - GIS analysis - GIS data base query
	5. Calculation of sediment volumes of different landform types (all hanging valleys)	Combine mean landform thickness with landform area: - GIS analysis
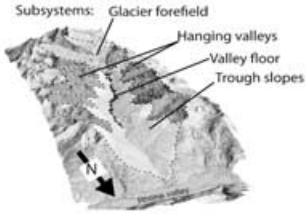	6. Modelling of sediment volume of remaining subsystem	
	- Main valley floor	DEM analysis using Sloping Local Base Level (SLBL)
	- Glacier forefield	Construction of parabolic profiles that resemble bedrock topography; subtract surface topography of bedrock topography
	- Trough slopes	Application of mean sediment thickness
	7. Calculation of sediment storage volumes for the entire valley	Combination of all subsystem volumes

used. Due to insufficient penetration depths of the geophysical instruments, geophysical soundings did not reveal the bottom of the rock glacier deposits. To differentiate between these two sediment bodies, mean rock glacier height along the front and lateral parts was subtracted from interpolated sediment thickness at these locations. Lateral and frontal height is frequently used to approximate rock glacier volumes (Barsch, 1977; Barsch and Jakob, 1998; Nyenhuis, 2006). Scenario I includes the subtracted, separated thickness information and Scenario II uses the entire sediment thickness without a differentiation of the two materials. This later scenario most probably overestimates the thickness of rock glaciers and underestimates till deposits. Other cases of overlapping landforms have not been considered and are expected to be insignificant for volume quantification. The debris volumes of rock glaciers are calculated assuming debris content of 40% for active types and 70% for inactive types (Barsch, 1996, Burger *et al.*, 1999, Arenson *et al.*, 2002). Sediment volumes of single landforms in this hanging valley were computed by combining sediment thickness and landform areas. To account for the steep terrain, real surface areas have been calculated from the DEM.

In order to determine sediment volumes of all hanging valleys, the resulting mean sediment thickness of each landform type obtained in the Hungerlitaelli were used as proxy values for the other hanging valley landforms. Mean sediment thickness values for each landform type were combined with landform areas to derive the volume (Step 5, Table I). This approach is based on the assumption that the landform number and distribution structure in the Hungerlitaelli is similar to the other hanging valleys, as revealed by the landform distribution analysis, and can be taken as representative for the entire Turtmann Valley. Lithology, tectonics, climate conditions, and topography provide similar conditions for debris accumulation in almost all hanging valleys of the Turtmann Valley. The Hungerlitaelli contains a typical and representative pattern of landform types, though protalus rock glaciers and alluvial deposits are not found in this area. However, as these landforms cover less than 2% of the entire Turtmann Valley area, their absence in the Hungerlitaelli was considered as not significant for the volume calculation of the entire catchment.

Storage quantification in the main valley trough subsystem

To estimate the volume of the trough filling a computational method developed by Jaboyedoff and Derron (2005), was used that excavates a DEM surface until an assumed glacial trough shape is created (Step 6.1, Table I). The method is based on the SLBL routine developed by Jaboyedoff *et al.* (2004). The SLBL approach uses the idea of a base level in geomorphology, defined as lower limit of subaerial erosion processes affected by fluvial erosion. Sea level is the general base level for all processes. However, local base levels above and below sea level, lakes or basin floors, exist as well. SLBL is defined as a surface above which rocks are assumed to be erodible by landslides, indicating a potential sliding surface. This surface is constructed by a virtual plane that joins all rivers. Jaboyedoff and Derron (2005) adapted the SLBL method in order to model the bedrock surface of the Rhone Valley, Switzerland. The new routine deepens a DEM surface by itera-

DOI: 10.1002/esp

tively calculating parabolas using a quadratic equation to describe glacial valley cross-sections proposed by Weehler (1984) and Li *et al.* (2001).

We used a DEM of 5 m resolution resampled from the 1 m HRSC dataset. To smooth the topography and reduce the effects of trees and houses in the calculation a Gaussian filter (5×5 cells window) was used. The SLBL routine allows the input of two parameters: (i) a mean curvature of the parabolas and (ii) a maximum depth of deepening. The parabola shape was adjusted to the mean profile curvature of the trough slopes. Profile curvature has been calculated using a 25 m DEM by applying the profile curvature algorithm developed by Evans (1980) with a 20×20 cell analysis window. To prevent overdeepening caused by the algorithm, a maximum depth of 75 m was used. This value that was chosen by comparing the very limited geophysical investigations published on glacial valley depths. An assessment of this depth is done at the end of the paper.

Storage quantification in the glacier forefield subsystem

A glacial forefield is the most dynamic part of an alpine sediment flux system. Very few studies ever quantified pro-glacial deposits (Small, 1987, Etzelmüller, 2000). The sediment fill of the glacier forefield subsystem in the Turtmann Valley was modelled using a similar approach as applied in the Hungerlitaelli hanging valley; however, no geophysical surveys have been performed here for validation (Step 6.2, Table I). Eight transects were placed across the forefield perpendicular to the forefield orientation. Three longitudinal profiles were used, one in the central forefield area and two along the ridge of the two large lateral moraines next to the glacier tongue. The glacier forefield terminates at a bedrock outcrop, where the dam is located today. This roche moutonée is incised by the draining meltwaters to a depth of 30 m. Assuming that the glacio-fluvial runoff was discharged on top of the bedrock surface, this incision depth is used as the maximum excavation depth of the forefield. The bedrock surface along the transects was constructed by fitting a parabola through the bedrock outcrop points towards the end and a central point of maximum depth. The parabolas were adjusted to fit estimated auxiliary points in order to represent an expected glacial trough. Additional, minimum depths of the lateral moraines were incorporated by measuring the height difference between the top of the moraine and the lowest neighbouring areas, most often drainage paths. Resulting transects have been used to interpolate the assumed bedrock surface. Before the volume was calculated, the area covered by the glacial tongue was erased from this interpolated surface. Thus, debris stored underneath the glacier is not considered here.

Storage quantification in the trough slopes subsystem

The sediment deposited on the slopes of glacial troughs has not been quantified in previous studies. The application of geophysical techniques on these deposits was not possible, thus the sediment volume of the trough slopes was estimated using an average sediment depth (Step 6.3, Table I). Main valley trough slopes in the Turtmann Valley are generally stable and covered with forest or alpine meadow. Bedrock outcrops frequently in the forest indicating a rather shallow sediment cover. Most streams have cut only shallowly into the debris cover (3–5 m) with some exceptions where debris flows have removed more material. Thus, a mean sediment thickness of 5 m is used to calculate a volume of the trough slope sides. All remaining areas above the trough slopes that are not included in the other subsystems have been quantified using an assumed average value of 3 m sediment cover. Most of these slopes are very steep (>30°) and only a thin debris cover is expected here, probably less than 3 m.

Calculation of denudation rates

Based on quantified debris volumes denudation rates (DR) have been calculated. These rates are based on the equation:

$$DR = SV \frac{\rho_b}{\rho_s A_d T} \quad (1)$$

including the sediment volume SV, dry bulk density of sediment ρ_s and of bedrock ρ_b, denudation area A_d and the time period of deposition T. A mean bedrock density ρ_b of 2·7 g/cm^3 for lithology of the Turtmann Valley (mica-schist, gneiss) is applied (data verified in laboratory experiment by Krautblatter, personal communication, 2009). Sediment density depends on the consolidation process, the composition of the deposit and the landform type. Density is assumed to be higher for glacial and fluvial deposits than for talus or rock glacier deposits. Debris density values determined or applied in other studies range from 1·5 to 2·6 g/cm^3 (Jäckli, 1957; Rapp, 1960; Hinderer, 2001; Sass and Wollny, 2001). As this study includes different types of storage landforms, a mean value of 2 g/cm^3 is used to calculate the denudation rates. Denudation rates have been calculated for different processes based on individual landforms with clearly distinguishable source areas. Four landform types have a distinctive source area that enables the calculation of denudation rates: (i) talus slopes, (ii) talus cones, (iii) block slopes and (iv) talus-derived active rock glaciers. Only landforms with well defined source areas have been used for denudation rate calculation, to reduce uncertainty of debris provenance. In case of block slopes the entire slope area was used as source area, assuming *in situ* sediment production. Rock glacier source areas include the talus slopes and the rock walls upslope, which may overestimate the denudation rates. Quantification of the denudational area is accomplished for single landforms using a watershed calculation algorithm in GIS. In the Turtmann Valley no dating information of sediments or landforms exists, so the period of deposition can only be assumed. The time of glacier maximum during the Younger Dryas phase has been dated in neighbouring valleys to around 9·5 ka BP (Bircher, 1983, Kelly *et al.*, 2004). To allow for a better comparability with other studies, a time of 10 ka was applied. The usage of a single time span for the calculation of denudation rates for different processes will be discussed later.

Results

Spatial distribution structure of storage landforms

A total of 593 sediment storage landforms have been mapped in the 14 hanging valleys of the Turtmann Valley (Figure 2). About 75% of this area is covered by sediment; the remaining parts of the surface include bedrock, glaciers and lakes. Sediment trapped in lakes and underneath glaciers is not considered here. More than 50% of the land surface covered by sediment is classified as slope deposits that include talus slopes (20%), talus cones (2·5%) and block slopes (28·7%). Moraine deposits cover around 37% of the land surface, followed by 11% covered by rock glaciers and 2% by alluvial sediments and rock fall deposits. Mean landform size ranges

DOI: 10.1002/esp

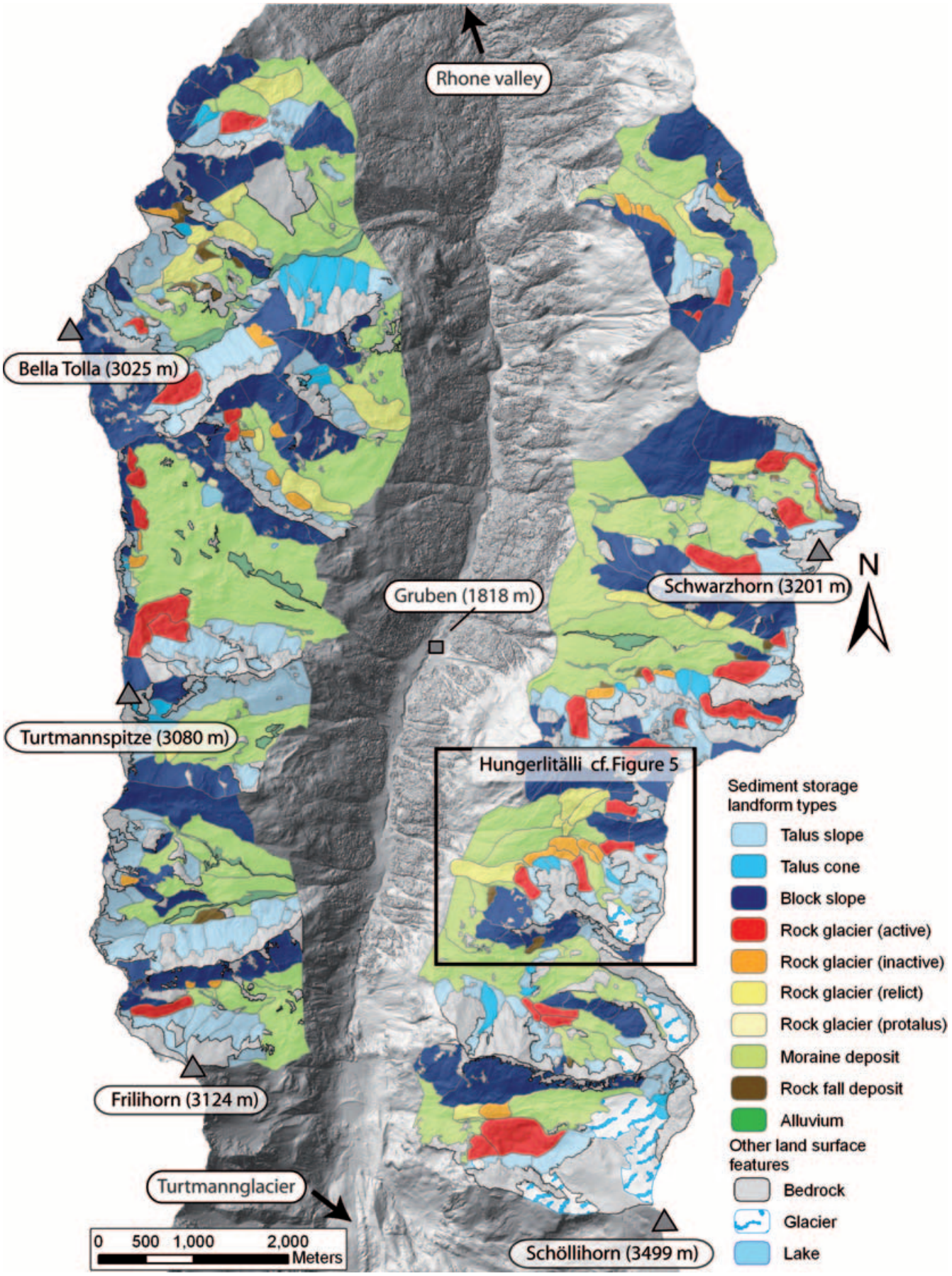

Figure 2. Distribution of storage landforms in the hanging valleys.

DOI: 10.1002/esp

Table II. Landform distribution and mean sediment thickness calculated in the Hungerlitaelli hanging valley

Landform type	Number	Real surface area (10^6 m^2)/ percentage of total	Mean sediment thickness (m)	
			Scenario I	Scenario II
Talus slope	18	0·46/17%	5·1	5·1
Talus cone	3	0·06/2%	16·0	16·0
Block slope	8	0·69/25%	5·8	5·8
Moraine deposits	9	0·60/21%	35·8	18·9
Rock fall deposits	1	0·02/<1%	20·2	20·2
Rock glacier (active)	5	0·21/8%	15·0	15·0
Rock glacier (inactive)	5	0·15/5%	11·1	29·7
Rock glacier (relict)	5	0·35/12%	7·6	29·0
Total debris covered area	54	2·54/100%		
Total hanging valley area		2·76		

Note: Between scenario I and II only values for moraine deposits, inactive and relict rock glaciers differ. Confer to explanation in the text.

from around 0·01 km^2 for alluvial deposits and protalus rock glaciers to more than 0·18 km^2 for moraine deposits, covering entire hanging valley floors (Table II).

The spatial distribution of the landforms shows a distinct relation to both altitude and aspect. The hanging valleys are located at altitudes between 2137 m and 3589 m a.s.l. The highest accumulation of debris is found at 3328 m. Higher altitudes are covered by slope landforms and active rock glaciers while lower parts of the hanging valleys are filled with moraine deposits, alluvium and relict rock glaciers. The orientation of the landform types, along its main axis, is directly influenced by the general orientation structure of the hanging valleys (cf. Figure 2). The hanging valleys are orientated from east to west, with openings towards the west or east according to their position relative to the main trough. Consequently, slopes and slope storages are mainly facing northern and southern directions, while moraine deposits cover lower and central parts of the valleys that are oriented from east to west and vice versa. The composition of these landforms within each of the hanging valleys shows a similarity with respect to relative area covered by each landform type. The proportion of surface area covered by the three dominant landforms (talus slopes, block slopes, moraine deposits) is very similar for most of the hanging valleys. Talus slopes cover between 15 and 25% of the hanging valley surface, while block slopes are found on 20 to 30% of the surface; moraine deposits are located on 35 to 45% of the catchment area. Rock glaciers, alluvium and rock fall deposits are not found in every hanging valley. The latter two cover less than 2% of the total hanging valley area.

A topological relationship between the landforms can be observed. Several toposequences, i.e. a succession of different landform types orientated in the direction of gravitational forces, can be distinguished. They form a sediment cascade when a coupling between these landforms exists. Among them, the most frequent cascade type observed is a coupling of rock faces and talus slopes. Other toposequences/sediment cascades are: rock face–talus slope–rock glaciers; moraine deposit–rock glacier; block slope–rock glacier.

Sediment volume of the Hungerlitaelli hanging valley

The modelling of the regolith thickness within the Hungerlitaelli hanging valley is based on the interpolation of 35 transects through the hanging valley. Transects were placed throughout the hanging valley and covered locations of geophysical profiling and additional places, where no geophysical surveying was performed. Detailed results of the geophysical surveys will not be presented here; we refer to Otto (2006) for more information on measurement characteristics and subsurface conditions.

Two profiles used in the interpolation will be discussed in detail in order to illustrate the interpolation procedure. The cross profile (Transect A, Figure 3) is located in the centre of the Rothorn cirque and spreads across a lateral moraine in the eastern part and active rock glacier at the western part of the profile. The longitudinal transect (Transect B, Figure 3) starts at a roche moutonée below the glacier front, following the thalweg into the centre of the hanging valley and continuing further down along the creek to terminate at the northern margin of a relict rock glacier at the outlet of the Hungerlitaelli hanging valley. Transect A was interpolated using a parabolic interpolation, which produces a smooth, rounded profile that resembles an idealized glacial trough. Towards the east end of the transect, the geophysical results reveal a shallow regolith thickness, with the bedrock surface located only 5–10 m below the surface. The depth of the central points is assumed, as no depth information is available here. However, below the lateral moraine a depth of 38 m is used based on ground penetrating radar (GPR) that did not detect the bedrock within the maximum penetration range of the radar waves at this location. Thus, this thickness is regarded as a minimum value for this location. The thickness of the rock glacier at the western part of the transect was assumed to be 35 m. This depth includes a height difference of the lateral rock glacier margin above the surface of about 10 m at this location and an assumed additional thickness of 25 m.

Transect B was interpolated using a linear interpolation to avoid over deepening of the modelled surface between the widely spaced points. The bedrock profile reveals a stepped surface in the upper part and a more smoothed surface in central parts of the hanging valley. Depths range between 5–10 m in the upper parts and up to 30 m in the valley centre. At the valley exit a sediment deposit of 15 m thickness was detected by geophysics.

The hanging valley has a total area of 2·7 km^2 with 92% being covered by debris. Debris thickness rises from a thin cover of less than 1 m on steep slopes and near bedrock outcrops to more than 50 m in the centre of the hanging valley

DOI: 10.1002/esp

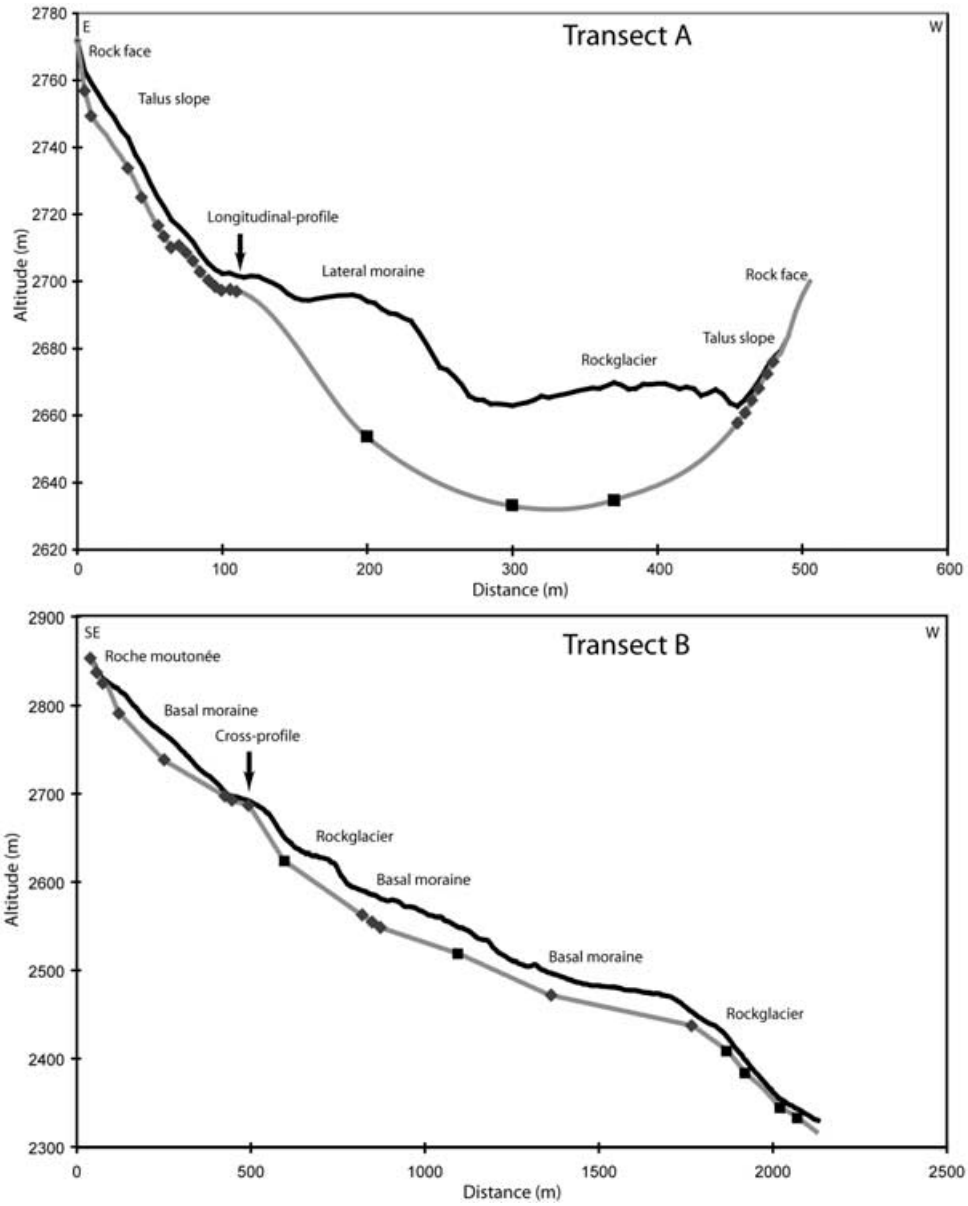

Figure 3. Bedrock transects through the Hungerlitaelli hanging valley. The black line represents the land surface, the grey line is the interpolated bedrock surface based on the diamonds and squares. Diamonds represent bedrock surface information derived from geophysical surveys; squares show points of assumed depth. Transect A, Cross profile through (vertical exaggeration: 3·75:1); Transect B, Longitudinal profile (vertical exaggeration: 4·2:1).

(Figure 4). Here, large inactive rock glaciers have overridden the glacial deposits.

Based on this interpolation, sediment volumes are calculated for each landform of the Hungerlitaelli hanging valley. The 54 landforms that store sediment include 18 talus slopes, three talus cones, eight block slopes, nine moraine deposits, five rock glaciers (active, inactive, relict) and one rock fall deposit. Talus landforms cover about 44% of the land surface, followed by rock glaciers (25%) and moraine deposits (22%).

Interpolated sediment thickness varies strongly within the different landform types (Table II). Talus slopes and block slopes have the thinnest debris cover of 1–18 m. As revealed by geophysical surveys these landforms often show a strong increase of debris depth down slope due to increased accumulation at the foot of slopes. Further, many upper locations of the hanging valley are included in this class, where the debris cover is estimated to be less than 1 m on average. Talus cones have a considerably higher sediment thickness due to their formative process. The channelling of debris input from above limits the accumulation area and hence increases the debris thickness. Moraine deposits show the largest scatter of thicknesses values. This class includes all types of moraine deposits, the wide-spread cover of basal moraine coverage as well as more linear and higher lateral deposits. Moraine deposits up to a thickness of 50 m have been recorded. The largest thickness values are calculated for inactive and relict rock glaciers in the centre of the hanging valley. However, this includes underlying glacial material as well. The inactive rock glaciers have a mean lateral height of 10–20 m, while relict rock glaciers rise between 5–10 m above the surrounding areas. Consequently, deposits of glacial origin are included in the rock glacier class producing a mean sediment thickness of 19–35 m that probably overestimates the 'real' rock glacier thickness by a factor of 2–4. Though, it has not been discussed in previous studies, rock glaciers are assumed to override neighbouring landforms without eroding its base. This assumption is backed up by the following observations: Coring in rock glaciers revealed a very heterogeneous internal structure with decreasing grain sizes downwards and underlying bedrock (Arenson *et al.*, 2002; Haeberli *et al.*, 2006). Geophysical

DOI: 10.1002/esp

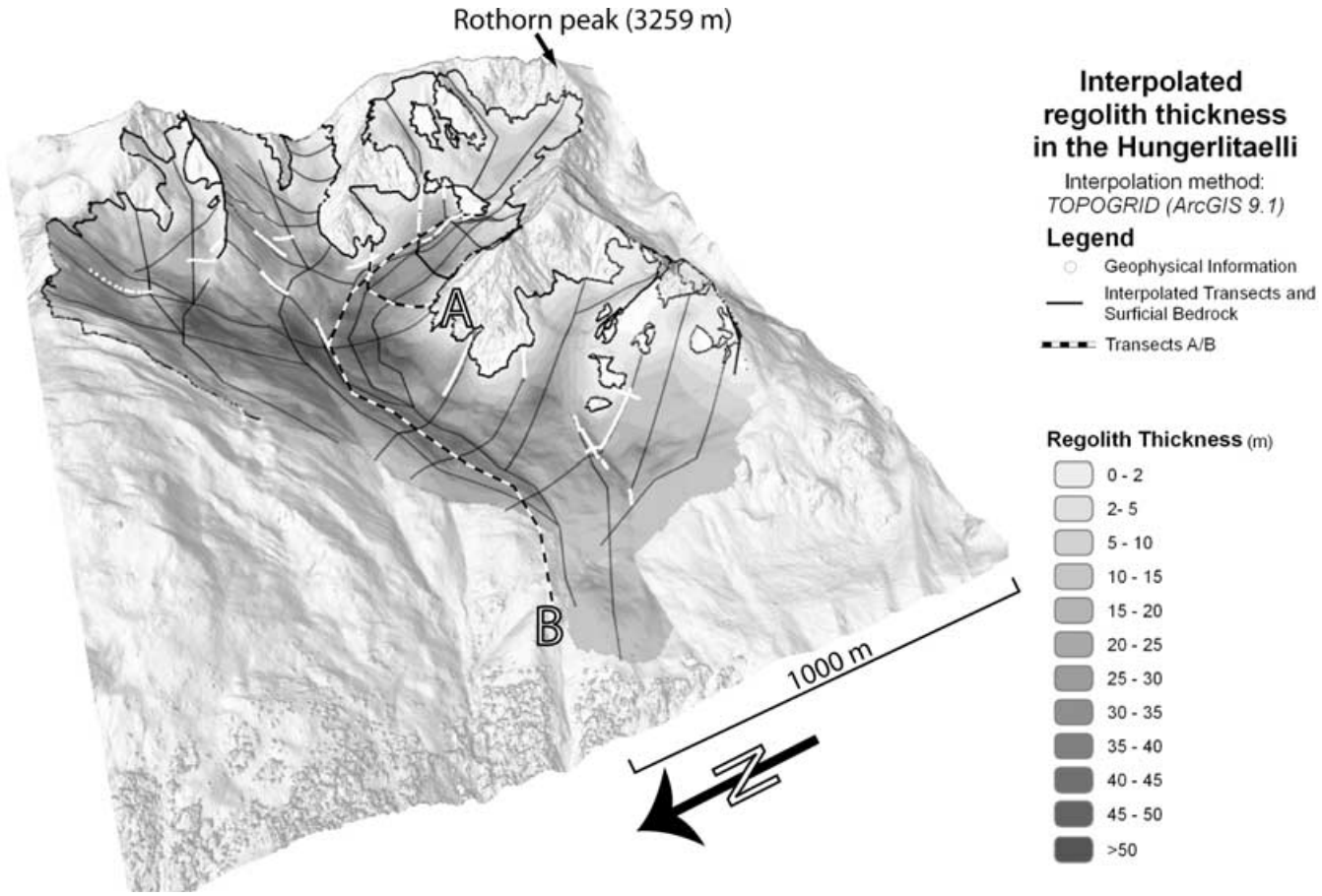

Figure 4. Interpolated regolith thickness and transects used for the interpolation in the Hungerlitaelli hanging valley. Geophysical profiles are shown in white. Black lines and white dots indicate the location of the transects. The dashed lines represent transect shown in detail in Figure 3.

investigations on the Reichenkar rock glacier (Austria) detected the presence of a non-deformed underlying till layer, that has been overridden by the rock glacier (Hausmann *et al.*, 2007). Measurement and modelling of rock glacier flow show a decrease of velocity towards the rock glacier base, often including a distinct shear zone (Arenson *et al.*, 2002; Kaab and Reichmuth, 2005).

The total sediment volume stored in the Hungerlitaelli hanging valley is $33{\cdot}7 \pm 8{\cdot}4{\times}10^6$ m^3. Of this volume 64% is stored in moraine deposit landforms. Talus slope deposits store about 20% of the total debris. Rock glaciers hold about 15% of the accumulated material using the corrected sediment thickness (Scenario II). The interpolated mean sediment thickness values from the Hungerlitaelli hanging valley will be used for an assessment of the debris volumes in the other hanging valleys of the Turtmann Valley.

Sediment volume of the entire Turtmann Valley

A total volume of $1005{\cdot}7 \pm 263{\cdot}4{\times}10^6$ m^3 (Scenario I) or $781{\cdot}3 \pm 207{\cdot}3{\times}10^6$ m^3 (Scenario II) is modelled for the four subsystems of the Turtmann Valley (Figure 5).

Compared to the other subsystems, the largest amount of sediment is stored in the hanging valleys (Table III). They contain more than 60% of the total volume. In contrast, the trough slopes subsystem that includes slopes above the trough and the remaining slopes outside the hanging valleys covers the largest area, but stores less material compared to the hanging valleys. However, they contribute 23–30% (Scenario I/II) to the total storage volume. The remaining 2 and 3% of material is currently stored in the glacial forefield and the main trough floor, respectively. The sediment volume/area ratio (*V/A*) reveals largest values for the valley floor with $22{\cdot}3$ m^3/m^2 followed by the hanging valleys with $17{\cdot}6$ to $11{\cdot}7$ m^3/m^2 (Scenario I/II). A similar sediment thickness is found in the glacier forefield ($11{\cdot}8$ m^3/m^2), while the trough slopes store only about $4{\cdot}2$ m^3 of sediment per square metre (Figure 5).

Within the hanging valleys, most of the sediment is stored in moraine deposits (75%/60%, Scenario I/II, respectively, Figure 6). Between 17% and 25% of debris is deposited at slopes (talus slope, talus cones, and block slopes), while rock glaciers store 5% to 13% of the total debris volume, according to Scenarios I and II, respectively. Alluvium and rock fall deposits include less than 2% of the debris volume in the hanging valleys (Figure 6).

Denudation rates

Quantification of sediment storage enables a calculation of denudation rates using Equation 1.

Denudation rates derived from talus cone volumes deliver the highest values ranging from $0{\cdot}5$ to $2{\cdot}6$ mm/a (Table IV). Block slope storage delivers denudation rates between $0{\cdot}6$ and $1{\cdot}8$ mm/a, while talus slope volumes indicates rate of $0{\cdot}2$ to $1{\cdot}0$ mm/a. The quantification of rock glacier volumes leads to denudation rates of $0{\cdot}1$ to $0{\cdot}7$ mm/a. For the entire Turtmann Valley a denudation rate of $1{\cdot}3$ and $0{\cdot}9$ mm/a (Scenario I/II) was calculated. In case of the hanging valleys this value

DOI: 10.1002/esp

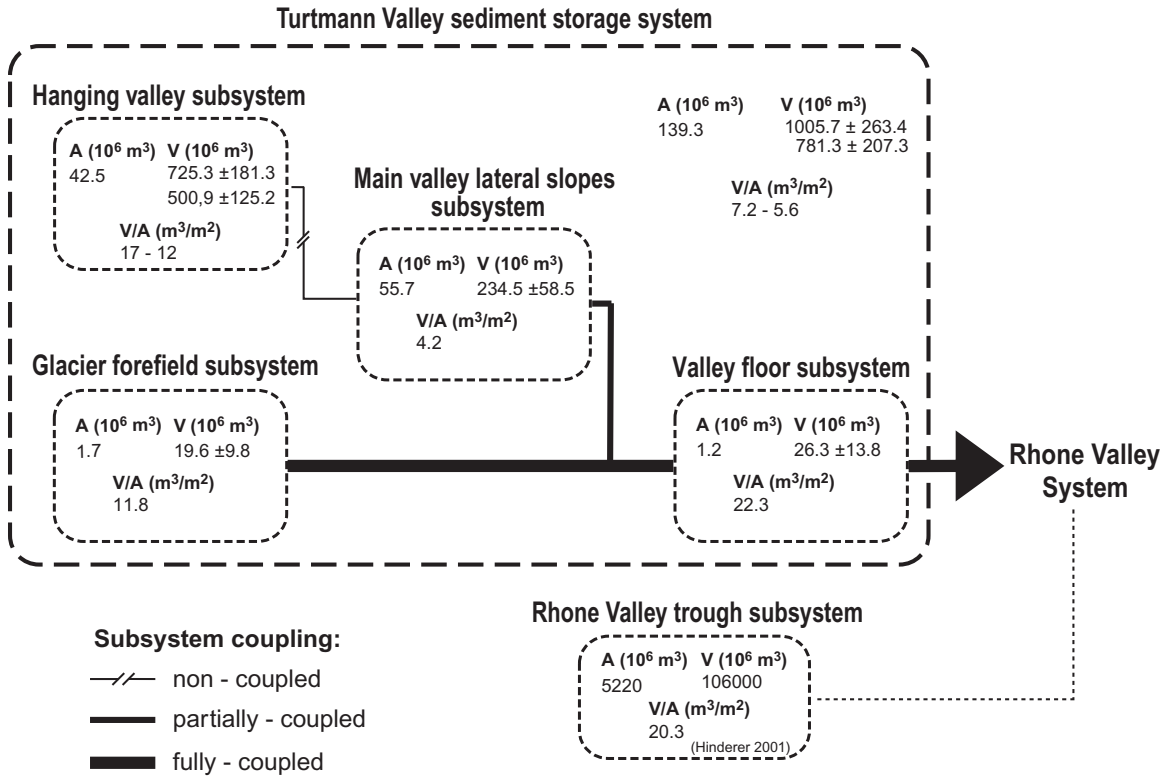

Figure 5. Sediment storage distribution and post-glacial subsystem coupling in the Turtmann valley. Coupling between glacier forefield and valley floor subsystem does not regard the dam construction in the 1950s. *A*, area, *V*, volume. Error margins include 25% error for hanging valleys and trough slopes and 50% error estimation for the glacier forefield and the main trough.

Table III. Sediment storage volume of the Turtmann valley subsystems

		Scenario I		Scenario II	
Subsystem	Area (10^6 m^2)	Volume (10^6 m^3)	Percentage of total (%)	Volume (10^6 m^3)	Percentage of total (%)
Hanging valleys	42·5	725·3 ± 181·3	72	500·9 ± 125·2	64
Glacier forefield	1·7	19·6 ± 9·8	2	19·6 ± 19·6	2
Valley floor	1·2	26·3 ± 13·8	3	26·3 ± 9·8	3
Trough slopes	55·7	234·5 ± 58·8	23	234·5 ± 58·8	30
Total	139·3	1005·7 ± 263·4	100	781·3 ± 207·3	100

increases almost two-fold delivering values of 2·3 (Scenario I) and 1·5 (Scenario II) mm/a. The debris volume stored in the glacier forefield represents significantly lower denudation rate of 0·1 mm/a. The calculation of denudation rates for the subsystems strongly depends on the delineation of the source area and the time span considered. Due to the lack of dating information, the approach assumes a single time span for all landforms which leads to large uncertainties in the calculation of denudation rates. This problem will be discussed later.

Potential Sources of Errors

A key issue of this study is the enlargement of the scale of investigation, compared to previous studies on sediment storage quantification. This implies the application of various assumptions, and consequently errors of different types that need to be considered. This means, that storage volumes presented here should reflect the order of magnitude that has to be expected in a catchment of this size, even some uncertainties might be large and cannot always be quantified.

Sources of error in the volume quantification include:

- Determination of mean sediment thickness values by extrapolating geophysical data.
- Use of mean thickness values for different landforms.
- Choice of main valley trough depth in the SLBL-modelling.
- Debris underneath glaciers and within lakes are not considered.

The approach of regionalization implies a major uncertainty of the presented quantification of sediment storage. Due to a lack of further data from other neighbouring hanging valleys it seems reasonable to use relatively accurate values from one representative hanging valley to calculate the overall sediment storage. Glacial history, climate, relief, present landform assemblages and geomorphometry do not differ significantly among all hanging valleys. At present no geophysical data is available from these areas to verify the modelling results.

A reasonable approach to crosscheck the results can be performed using the Hungerlitaelli data. Here, sediment thickness has been determined using geophysical methods at single landforms that provide highest accuracy (error < 10%). By

DOI: 10.1002/esp

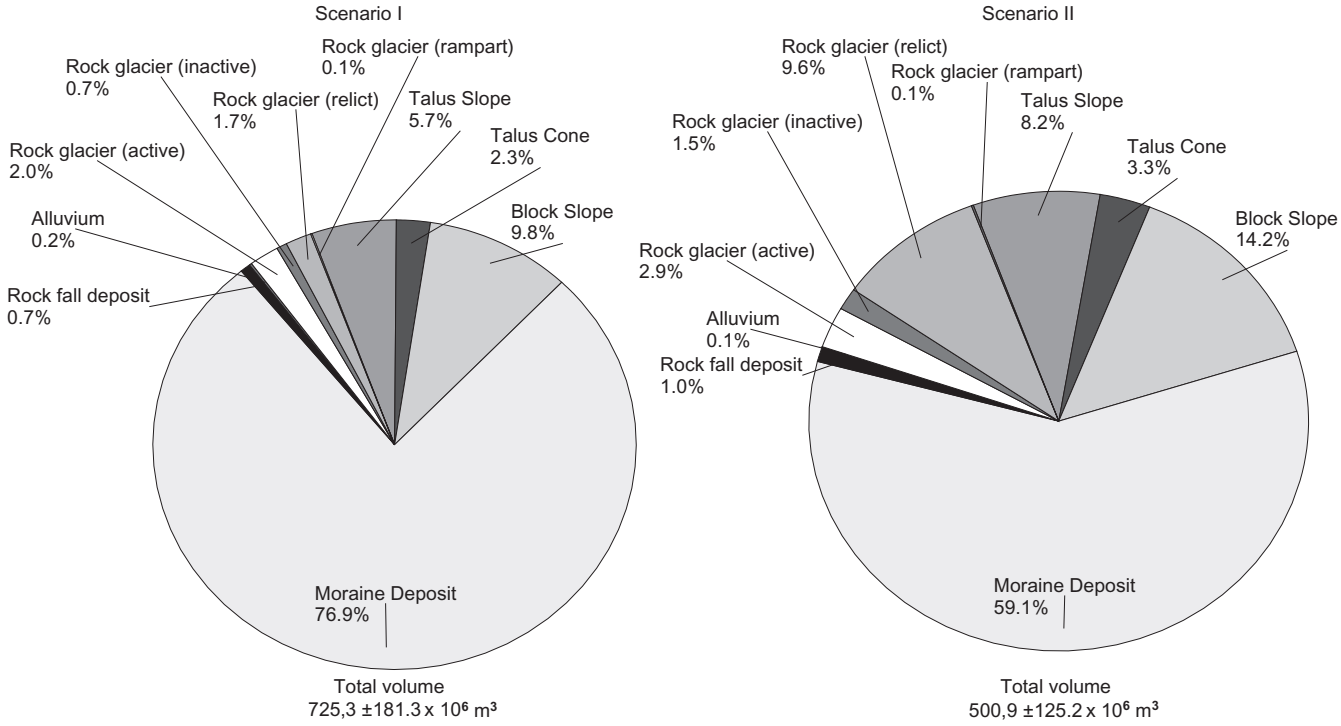

Figure 6. Distribution of sediment volumes per landform type in the hanging valleys calculated for scenario I (left) and II (right).

Table IV. Denudation rates derived from single landform volumes (estimated error margin 20%)

	Denudation rate (mm/a)		
Landform	Minimum	Mean	Maximum
Talus slopes	0·2 ± 0·04	0·7 ± 0·14	1·3 ± 0·26
Talus cones	0·6 ± 0·12	2·2 ± 0·44	3·1 ± 0·62
Block slopes	0·8 ± 0·16	1·4 ± 0·38	2·3 ± 0·46
Rock glaciers	0·12 ± 0·02	0·62 ± 0·12	1·8 ± 0·36

extrapolation additional thickness information was generated for other landforms within the hanging valley. The uncertainty introduced by this procedure is difficult to determine and will vary at different locations in the Hungerlitaelli due to variable erosion and deposition rates. Hence, the sediment thickness calculated can be over- or under-estimated with an estimated error of 20%.

Sediment volumes in the Hungerlitaelli have been calculated from the product of a sediment thickness interpolation (Figure 4) and the real surface area in GIS on a pixel basis. For Scenario II, that uses non-adjusted mean values of sediment thickness (in Scenario I material stored in rock glaciers is separated from overlapping moraine deposits), we can compare the volume generated using GIS with the volumes derived using mean thickness values. The resulting landform volumes are about 10–25% smaller when derived from mean thicknesses compared to GIS modelling results (Table V). Only volumes of talus slopes and relict rock glaciers are approximately 10% and 19% larger, respectively. This reflects the large scatter in sediment thickness values within one landform. According to this approach, the entire sediment volume quantified in the Hungerlitaelli using thickness values from Scenario II is underestimated by 10%. We estimate the error of volume calculation for all hanging valleys to be not greater than 25%. The scatter of thickness, calculated on a pixel basis is obviously large for some landforms (see Figure 7). However, the mean values used in Scenario II are close to the median for most of the landform types. The variation of the scatter between landform types is generated by the evolutionary process, shape and the location of the landform. Talus slopes, for example, have a thin sediment cover of a few centimetres at the upper slope and can accumulate ten's of metres of debris at the foot slope within one landform. For comparison, we compiled information on landform thickness in alpine areas from previous studies. The data reveals that landform thickness in general show a large scatter between the different objects, types and locations (Table VI). Even though high heterogeneity of landform depths exists, we conclude that the application of mean sediment thickness is a reasonable approach to generate a first-order estimation of sediment storage of single landforms in large catchments.

To model main trough sediment fill, we created an ideal U-shaped valley floor using the SLBL routine. The routine requires a maximum depth in order to generate the U-shape. Here, a depth of 75 m was chosen based on previous data of glacial trough depths in the Alps. However, these values enclose a very broad range between large valleys like the upper Rhone Valley with a catchment size >5000 km^2 and maximum depths up to 900 m (Finckh and Frei, 1991; Pfiffner *et al.*, 1997; Rosselli and Olivier, 2003) and smaller valleys of sizes <40 km^2 with a maximum depth of up to 30 m (Schrott *et al.*, 2003). Consequently, the chosen value of valley depth is a rough estimate that we consider to be realistic within the depth range of ±50%. More accurate data on glacial valley fill depth is required derived from geophysics in order to verify this assumption.

The debris stored in small pro-glacial lake and several ponds and underneath glaciers is not considered in the quantification. These features cover less than 9% of the total catchment area (glaciers approximately 13 km^2 and lakes 0·1 km^2). The contribution to the sediment storage volume is regarded to be insignificant, especially when considering the overall number of uncertainties of the study.

DOI: 10.1002/esp

Table V. Volumes of landform types in the Hungerlitaelli hanging valley calculated using mean thickness values and by GIS modelling

	Area (m^2)	Mean thickness, Scenario I (m)	Volume Scenario I (10^6 m^3)	Mean thickness, Scenario II (m)	Volume, Scenario II (10^6 m^3)	Volume, GIS model (10^6 m^3)	Diff. vol. I/GIS (%)	Diff. vol. II/GIS (%)
Talus slope	375950	5·1	1·92	5·1	1·92	1·73	9·7	9·7
Talus cone	51675	16	0·83	16	0·83	0·96	–15·7	–15·7
Block slope	558025	5·8	3·24	5·8	3·24	4·07	–25·9	–25·9
Moraine deposit	550275	35·8	19·70	18·9	10·40	12·82	34·9	–23·3
Rock fall deposit	13700	20·2	0·28	20·2	0·28	0·31	–10·8	–10·8
Rock glacier (active)	185825	15	2·79	15	2·79	3·46	–24·2	–24·2
Rock glacier (inactive)	137675	11·1	1·53	29·7	4·09	4·79	–213·4	–17·1
Rock glacier (relict)	319675	7·6	2·43	29	9·27	7·78	–220·4	16·0

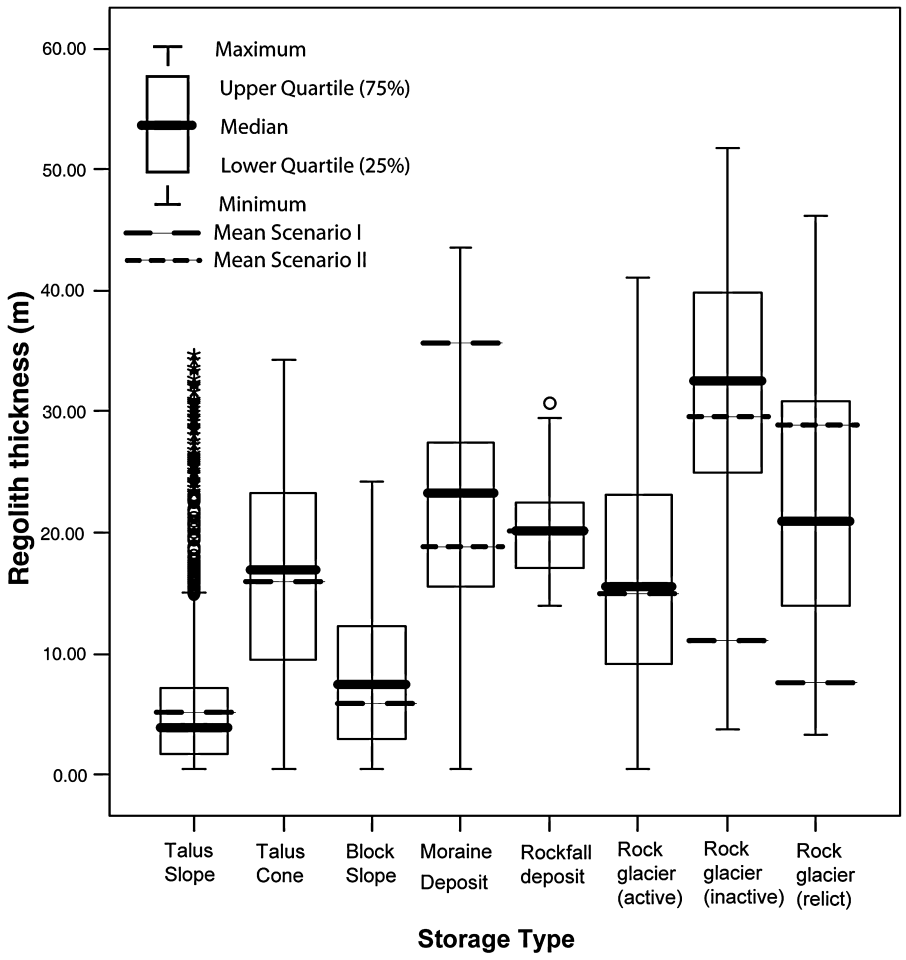

Figure 7. Box plot of storage landform sediment thickness derived from GIS modelling in the Hungerlitaelli. The single marks represent extreme values that lie outside a range of more than 1·5 box length away from the upper quartile.

Calculation of denudation rates based on storage volumes enables a comparison of the applied method to other similar studies. However, several difficulties arise from Equation 1. Main sources of error in the calculation of the denudation rates include:

- Delineation of the denudation, or source area of a landform/process.
- Quantification of sediment volumes.
- Uniform time of deposition.
- Uniform material bulk density.

The determination of the source area is not always possible, as it may have changed in time and/or no trace of the actual process area is left. For example, quantification of the source area of a basal moraine deposit depends on knowledge about the timing of glacial retreat. Unfortunately, no dating information is available in the Turtmann Valley to fulfil this task. Denudation area quantification is more easily performed for landforms like talus slopes, talus rock glaciers or talus cones whose source area is more clearly definable. Furthermore, calculating mean denudation rates for entire catchments remains difficult with respect to the delineation of the denudational area. Two possible solutions can be imagined: Firstly, the usage of the current area of surface bedrock; secondly, the usage of the entire catchment area including the storage area. The first approach underestimates the denudational area, while the latter one tends to overestimate it. Unfortunately, most of the studies quoting denudation rates for entire catchments do not mention the type of source area used.

DOI: 10.1002/esp

Table VI. Sediment thickness of selected landform types published previously

Location	Reference	Method	Sediment thickness (m)
Talus slopes/cones			
Bavarian Alps (Germany)	Sass and Wollny (2001)	GPR	10–15
Lechtaler Alp (Austria)	Sass (2006)	GPR, SR, ER	25
Bavarian Alps (Germany)	Hoffmann and Schrott (2002)	SR	7–23·5
South Wales (UK)	Curry and Morris (2004)	Geometry	4–7
Snowdonia, North Wales (UK)	Sass *et al.* (personal communication)	GPR	8–10
Blockslopes			
Various (UK)	Ballantyne and Harris (1994)	Not specified	0·6–3·5
Rockglaciers			
Swiss Alps (Switzerland)	Barsch (1977)	Estimation based on height of frontal lobe	30–100
Khumbu Himalaya (India)	Barsch and Jacob (1998)	Estimation based on height of frontal lobe	11–41
Himalaya, Karakorum (India, Pakistan)	Owen and England (1998)	Estimation	>15
Various	Burger *et al.* (1999)	Various	8–120
Swiss Alps (Switzerland)	Arenson *et al.* (2002)	Borehole drilling	>63
Turtmann valley (Switzerland)	Nyenhuis (2006)	Estimation based on height of frontal lobe	3–38
Alluvial deposits			
Bavarian Alps (Germany)	Schrott *et al.* (2003)	Coring, SR	3–10

Note: GPR, ground penetrating radar; SR, seismic refraction; ER, electric resistivity.

Table VII. Denudation rates calculated for entire drainage basins

Location	Denudation rate (mm/a)	Time period	Source
Turtmann Valley (Switzerland)	0·62–1·87	Post-glacial (10 ka)	This study
Hungerlitaelli (Switzerland)	1·42–2·64	Post-glacial (10 ka)	This study
Walensee (Switzerland)	>1·5	15 ka	Müller (1999)
Upper Rhone Valley (Switzerland)	0·95	Late + post-glacial	Hinderer (2001)
Alps (mean)	0·62	Late + post-glacial	Hinderer (2001)
Bündner Rhine (Switzerland)	0·581	Quaternary	Jäckli (1957)
Langental (Italy)	1·1	Post-glacial	Schrott and Adams (2002)
Reintal (Germany)	0·3	Post-glacial	Hufschmidt (2002)
Alps (mean)	0·13	Present day	Hinderer (2001)
Rhone/Brig (Switzerland)	0·35	Present day	Schlunegger and Hinderer (2003)
Rhone/Port de Scex (Switzerland)	0·15	Present day	Schlunegger and Hinderer (2003)
Vispa/Visp (Switzerland)	0·72	Present day	Schlunegger and Hinderer (2003)

Furthermore, it is often not stated whether the planimetric surface, or the real surface area was used, which is especially of importance in high relief terrains like mountains. In the Turtmann Valley the real surface is about 40 km^2 larger than the commonly used planimetric surface. The difference between current bedrock area and the total valley surface is about 100 km^2 resulting in denudation rates decreased by a factor of 3·5.

Time plays an important role in the calculation of denudation rates, especially for single landforms/processes. The time span applied represents the assumed duration of denudation and hence is governed by the time of deglaciation and the beginning of landform formation. A time period for total denudation of 10 ka was assumed, because no dating information concerning deglaciation is available for the study area. However, this uniform time span for all landforms yields the largest uncertainties for the quantification of denudation rates. The timing and duration of processes and the process intensity most probably changed between different process types and are surely idiographic from landform to landform. A uniform time of 10 ka thus is probably too long for talus slope development, or rock glacier activity, landforms whose formation started after the deglaciation. The resulting denudation rates are therefore too low, compared to a shorter time of landform evolution. This might explain the significantly lower denudation rates of rock glaciers compared to for example the study of Barsch (1977) (compare Tables VII and VIII), though Barsch also uses (based on assumptions) larger mean rock glacier thicknesses compared to the Turtmann Valley. While the onset of deglaciation can be more easily determined by dating techniques, the time of process termination and variations in process activity is more difficult to determine. However, this is an inherent problem of denudation rate calculation and should be addressed more frequently in comparable studies.

The application of one uniform bulk density for different types of landforms introduces another source of error. The value chosen (2 g/cm^3) will probably better represent high density deposits like moraines and valley fill deposits, but underestimate the denudation rate of for example rock glaciers and talus deposits with large grain sizes and ground voids.

Some of the errors reported for calculation of denudation rates may balance out or vary between individual landforms, which complicates the determination of one single error margin. We estimated a general error of 20% for the calculated denudation rates.

The various errors discussed are intrinsic to many similar sediment budget studies (Hinderer, 2001). Despite these discussed errors the proposed approach of volume quantification can be regarded as a feasible approximation considering the

DOI: 10.1002/esp

Table VIII. Denudation rates for different landforms/process types (various time periods used)

	Rock wall retreat/denudation rate (mm/a)			
Landform type/location	Minimum	Mean	Maximum	Source
Talus slopes/rock fall				
Turtmann Valley (Switzerland)	0·2	0·7	1·3	This study
Kärkevagge (Sweden)	0·04	–	0·15	Rapp (1960)
Reintal (Germany)	0·1	–	1·0	Hoffmann and Schrott (2002)
Bavarian Alps (Germany)	0·06	0·28	0·73	Sass and Wollny (2001)
Talus cones /rock fall:				
Turtmann Valley (Switzerland)	0·6	2·2	3·1	This study
Lechtaler Alps (Austria)	0·5		0·8	Sass (2007)
Central Himalaya (Nepal)	3·2	–	15·6	Wantanabe *et al.* (1998)
Nanga Parbat (Pakistan), (alpine fans)	0·3	2·5	7·0	Shroder *et al.*(1999)
Block slopes/*in situ* weathering:				
Turtmann Valley (Switzerland)	0·8	1·4	2·3	This study
Rock glaciers/peri-glacial creep				
Turtmann Valley(Switzerland)	0·12	0·62	1·8	This study
Swiss Alps (Switzerland)	0·5	2·5	4·6	Barsch (1977)
Sierra Nevada (USA)	0·8	–	1·9	Höllermann (1983)
South Tirol (Italy)		0·5		Höllermann (1983)
Middle Asia	0·4	–	0·7	Gorburnov (1983)
West Greenland (Denmark)	2	–	5	Humlum (2000)

size of the study area and the number of landforms addressed. Even if a general error of 50% for the different subsystem volumes is assumed, the order of magnitude remains reasonable and the variations do not affect our conclusions.

Discussion

Distribution of landforms and sediment storage

The study delivers the distribution of sediments and the order of magnitude of sediment volume in the Turtmann Valley, Swiss Alps. More than 65% of sediment is stored in hanging valleys that are considered to be closed systems with respect to coarse sediment transfer. Due to topographic and geomorphologic conditions, they have been decoupled from the main valley sediment flux system and do not contribute to sediment output (Figure 5). Apart from fluvial discharge, almost no geomorphic process delivers material to hanging valley outlets. Few, undated, but most likely early Holocene/late Pleistocene relict rock glacier can be found below the hanging valley outlets on the trough slopes.

The hanging valleys are characterized by gravitational or peri-glacial processes and sediment transfer occurs only on slopes and upper locations. Sediment cascades are not very well developed and stretch over short distances. The large volume of sediment in the hanging valleys can be explained by long process duration and more importantly by a lack of material output. Sediment export operates along narrow corridors on the main valley trough slopes, for example in creeks, debris flow channels and avalanche tracks.

Glacial deposits dominate the sediment distribution in the hanging valleys. However, approximately 50% of the sediment cover is composed of talus slopes. Rock glaciers that rework glacial and talus material store significant amounts of material as well. They are characterized by a large sediment thickness and a deposition in very confined areas.

The sedimentary fill of the main valley floor is composed of material deposited by different processes operating at different time scales. Though, the composition of the valley fill is not differentiated in this study, the influence of glacial, glaciofluvial, and gravitational processes can be observed in the landforms within the valley floor. The latter processes include debris flows and snow avalanches originating from the lateral slopes that form large cones in the valley floor. Several levels of fluvial terraces along the Turtmann creek reflect variable discharge conditions during the Holocene (Otto and Dikau, 2004).

The glacier forefield subsystem and the main valley floor subsystem have been fully coupled since the end of Pleistocene. In the upper part of the main valley, bedrock depressions have been filled with sediments. The main trough was filled after a large rock fall event in the lower part of the valley that blocked the course of the creek and resulting in the sedimentation of the current valley floor level. The relict rock fall deposit has not been dated, but is considered to be of early Holocene age due to the occurrence of well developed soils at the surface (Otto and Dikau, 2004). However, sediment discharge from the glacier forefield and the main valley floor took place during most of the post-glacial period. The comparably high sediment cover per area in the main valley floor can be explained by the high process intensity of glacial and glaciofluvial erosion and a temporary decoupling of the subsystem that created a sedimentary sink. The sediment volume of the main valley floor has not been verified by geophysical sounding or coring and includes the largest uncertainties in this study. Furthermore, the calculated deposits in the main floor and the glacier forefield subsystems represent only a fraction of the total material eroded since glacial retreat. In the recent past, the glacier subsystem was decoupled from the main valley by the construction of a dam in the glacier forefield in the 1950s and the melt waters are transferred to a neighbouring valley for energy production. Since then, sediment discharge from the Turtmann Valley is confined to remobilization of deposits by water originating from the hanging valleys only.

Material stored on lateral slopes of the main valley contributes approximately 20% of the total valley storage. These deposits include glacier depositions in former lateral moraines and, at higher locations, talus deposits. Most of these areas are covered by vegetation, forest, scrub or grass, and do not contribute to the sediment flux system. Only along small corridors material is removed from these areas (see earlier).

DOI: 10.1002/esp

Comparison with previous studies on alpine sediment flux

Previous studies quantified the sediment storage in catchment about an order of magnitude smaller (1–27 km^2) than the Turtmann Valley (110 km^2) (Rapp, 1960; Caine, 1986; Schrott and Adams, 2002; Schrott *et al.*, 2002). In contrast, Jäckli (1957) and Jordan and Slaymaker (1991) investigated drainage basins which are much larger (4000–5000 km^2). The study bridges a gap between previously studied small meso scale valleys (<30 km^2) and macro scale drainage basins (>4000 km^2).

It has to be pointed out, apart from the works of Jäckli (1957) and Caine (1986) no comparable study has been carried out in an environment where rock glaciers have such a strong role in the sediment flux system. Comparing preceding studies on sediment flux, a change of process domains that predominates the sediment flux and storage situation can be observed with scale. Talus processes and storage are the most important sediment flux agents observed in small scale studies (Rapp, 1960; Caine, 1986; Schrott and Adams, 2002; Schrott *et al.*, 2003), while fluvial processes and glaciofluvial storage take over in large basins (Jäckli, 1957; Jordan and Slaymaker, 1991). This observation fits with the model of paraglacial evolution by Church and Slaymaker (1989) that describes a shift of sediment yield from uplands to lowlands, which includes a change of the dominant process domain.

In the Turtmann Valley sediment storage is dominated by glacial and glaciofluvial deposits. Thus, the valley has already reached the critical size where process domains and storage types change from gravitational to glacial and glaciofluvial processes. Paraglacial reworking is restricted to the glacial forefields of the Turtmann glacier and the small hanging valley glaciers. Remnants of previous paraglacial landform evolution are given by the numerous inactive and relict glacier-derived rock glaciers. Fluvial processes and debris flows play only a minor role in the sediment storage system of the hanging valleys. This may be caused by dry, inner-alpine climatic conditions with high summer temperatures, increased summer evaporation and large infiltration capacity of the mostly coarse debris of crystalline rocks. Furthermore, periglacial conditions evoke significant storage of water in the ground at higher altitudes. However, along the main valley floor and the main trough slopes, debris flows and avalanches as well as fluvial processes influence the sediment transport.

Denudation rates and post-glacial landform evolution

To evaluate the order of magnitude of the sediment volume, we converted volumes into denudation rates. These were compared with other data from the Alps (Tables VII and VIII). Rates of denudation calculated from sediment deposits can represent mean numbers of long-term erosion. A range of values between <1 and 2 mm/a have been generated for post-glacial period in the Alps (Tables VII and VIII). The mean denudation rate of the entire Turtmann Valley (0·67–0·97 mm/a) represents the lower end of the range of published data. The more accurate volumes of the Hungerlitaelli deliver a mean denudation between 1·14 and 2·11 mm/a. Present-day fluvial denudation rates (mechanical denudation) compiled by Schlunegger and Hinderer (2003) are significantly lower, strongly depending on the measurement position within the drainage basin or drainage basin characteristics. Basins with strong glaciofluvial impact like the Rhone river above Brig, or the Vispa creek, one valley to the east of the Turtmann Valley, show larger denudation rates (0·35–0·72 mm/a) compared to the Rhone river at Lake Geneva (0·15 mm/a). However, these present-day rates are strongly influenced by the wide spread construction of dams in Swiss rivers that cause sediment trapping.

The denudation rates converted from single landform volumes in the Turtmann Valley are within a range of 0·2 and 2·6 mm/a. This indicates that the applied time span of 10 ka probably overestimates the duration of landform accumulation and delivers mean rates that are underestimated.

Sediment storage and mountain uplift

The Turtmann Valley is located within a zone of highest uplift rates in the Alpine orogen. The upper Valais experiences uplift rates of up to 1·6 mm/a (Schlunegger and Hinderer, 2001). Current concepts of tectonic landform evolution of Alpine type orogens consider uplift as isostatic rebound to sediment removal by erosion (Molnar and England, 1990; Schlunegger and Hinderer, 2001). However, these concepts do not account for sediment storage within the upper areas of orogens. Our study shows that current processes do not remove sediments from the hanging valleys, while large amounts of glacial and non-glacial deposits are still stored in the upper parts. Fluvial and glaciofluvial processes dominate the sediment removal and transport along the large alpine valleys and remobilize the glacial deposits. The current land surface however, contains sedimentary traps even in the upper parts resulting from the imprint of Pleistocene glaciations on the bedrock surface. Under current climate conditions these deposits are only remobilized at very steep locations, or at the borders of hanging valleys and cirques. Erosional processes in the hanging valleys, like rock fall, debris flows or glacial erosion, operate within closed subsystems that are separated from the main sediment flux system along the main valleys. Thus, while the orogen might be responding to sediment removal from the main valleys, in the upper parts sediment is accumulating by current processes.

Conclusion

For the first time, a detailed quantification of different high alpine storage types was achieved in a catchment of this size (110 km^2), exemplified in the Turtmann Valley, Swiss Alps. To tackle catchment size and the high number of depositional landforms a subdivision into sedimentation subsystems was performed and a combination of different methods has been applied. A total volume of $1005{\cdot}7\times10^6$ m^3 (Scenario I) or $781{\cdot}3\times10^6$ m^3 (Scenario II) is currently deposited in the Turtmann Valley, according to Scenarios I and II, respectively. Over 60% of this volume is stored in hanging valleys followed by deposition on the main valley slopes, in the main valley trough and the glacier forefield. In the hanging valleys, largest depositional volumes resulted from glacial processes, followed by deposits on slopes (talus slopes, talus cones, block slopes). Even though the approach includes a number of assumptions that introduce partly unquantifiable sources of errors, we consider the results reliable in providing an order of magnitude of sediment volume stored in this valley.

From the observed distribution of sediment storage in the Turtmann Valley we can conclude that hanging valleys represent important temporary sediment sinks that are decoupled from the main sedimentary systems with respect to coarse sediments. The localization and quantification of sediment deposits in alpine catchments plays a key role in the understanding of past and present sediment dynamics and should

DOI: 10.1002/esp

be considered in landscape evolution models. Bearing in mind the observed and predicted reactions of alpine areas to environmental and climate change we urge for a more detailed understanding of sediment storage in order to enhance the management of sediment flux and landform change in the future. The challenge for storage quantification in large drainage basins is to integrate between more accurate methods like geophysics and more efficient remote sensing and GIS modelling approaches to cope with large areas and the inherent complexity of depositional landforms. This integration requires applicable proxies for deposition volumes, for example from landform geomorphometry, that help to bridge between the different scales and methodological accuracies. We conclude that, given the size and nature of the catchment and the large number of different landforms considered, the study represents a best practice approach to deliver sediment volumes for high alpine environments.

Acknowledgements—The study was part of the Research Training Group 437 – Landform, a structured and variable boundary layer at the Department of Geography, University of Bonn, Germany. The financial support from the Deutsche Forschungsgemeinschaft (DFG) for Jan-Christoph Otto is gratefully acknowledged. We thank two anonymous reviewers and Arjun Heimsath for helpful comments and suggestions on an earlier version of the manuscript.

References

Arenson L, Hoelzle M, Springman S. 2002. Borehole deformation measurements and internal structure of some rock glaciers in Switzerland. *Permafrost and Periglacial Processes* **13**: 117–135.

Ballantyne CK. 2002. Paraglacial geomorphology. *Quartenary Science Reviews* **21**: 1935–2017.

Ballantyne CK. 2003. Paraglacial landform succession and sediment storage in deglaciated mountain valleys: theory and approaches to calibration. *Zeitschrift für Geomorphologie Suppl.* **132**.

Ballantyne CK, Harris C. 1994. *The Periglaciation of Great Britain*. Cambridge University Press: Cambridge.

Barsch D. 1977. Nature and importance of mass-wasting by rock glaciers in alpine permafrost environments. *Earth Surface Processes* **2**: 231–245.

Barsch D. 1996. *Rockglaciers – Indicators for the Present and Former Geoecology in High Mountain Environments*. Springer-Verlag: Heidelberg.

Barsch D, Jakob M. 1998. Mass transport by active rockglaciers in the Khumbu Himalaya. *Geomorphology* **26**: 215–222.

Bearth P. 1978. Geologischer Atlas der Schweiz, Blatt 1308 St. Niklaus, 1:25000. Birkhäuser: Basel.

Bircher W. 1983. Zur Gletscher- und Klimageschichte des Saastales. Glazialmorphologische und dendroklimatologische Untersuchungen. Physische Geographie 9. Geographisches Institut: Zurich.

Burger KC, Degenhardt JJ, Giardino JR. 1999. Engineering geomorphology of rock glaciers. *Geomorphology* **31**: 93–132.

Caine N. 1986. Sediment movement and storage on alpine slopes in the Colorado Rocky Mountains. In *Hillslope Processes*, Abrahams AD (ed.). Allen & Unwin: London; 115–137.

Caine NT. 1974. The geomorphic processes of the alpine environment. In *Arctic and Alpine Environments*, Ives JD, Barry RG (eds). Methuen: London; 721–748.

Campbell D, Church M. 2003. Reconnaissance sediment budgets for the Lynn Valley, British Columbia: Holocene and contemporary time scales. *Canadian Journal of Earth Science* **40**: 701–713.

Church M, Ryder JM. 1972. Paraglacial sedimentation: a consideration of fluvial processes conditioned by glaciation. *Geological Society of America Bulletin* **83**: 3059–3071.

Church M, Slaymaker O. 1989. Disequilibrium of Holocene sediment yield in glaciated British Columbia. *Nature* **337**: 452–454.

Cossart E, Fort M. 2008. Sediment release and storage in early deglaciated areas: towards an application of the exhaustion model from the case of Massif des Ecrins (French Alps) since the Little Ice Age. *Norsk Geografisk Tidsskrift – Norwegian Journal of Geography* **62**: 115–131.

Curry AM. 1999. Paraglacial modification of slope form. *Earth Surface Processes and Landforms* **24**: 1213–1228.

Curry AM, Morris CJ. 2004. Lateglacial and Holocene talus slope development and rockwall retreat on Mynydd Du, UK. *Geomorphology* **58**: 85–106.

Dadson SJ, Church M. 2005. Postglacial topographic evolution of glaciated valleys: a stochastic landscape evolution model. *Earth Surface Processes and Landforms* **30**: 1387–1403.

Etzelmüller B. 2000. Quantification of thermo-erosion in pro-glacial areas – examples from Svalbard. *Zeitschrift für Geomorphologie N.F.* **44**: 343–361.

Evans IS. 1980. An integrated system of terrain analysis and slope mapping. *Zeitschrift für Geomorphologie, Supplement Band* **80**: 274–295.

Finckh P, Frei W. 1991. Seismic reflection profiling in the Swiss Rhone valley. Part I: seismic reflection field work, seismic processing and seismic results of the Roche-Vouvry and Turtmann and Agarn lines. *Eclogae Geologicae Helvetiae* **84**: 345–357.

Fryirs K, Brierley GJ. 2001. Variability in sediment delivery and storage along river courses in Bega catchment, NSW, Australia: implications for geomorphic river recovery. *Geomorphology* **38**: 237–265.

Gorburnov AP. 1983. Rock glaciers of the mountains of middle Asia. Proceedings of the 4th International Conference on Permafrost; 359–362.

Graf WL. 1970. The geomorphology of the glacial valley cross section. *Arctic and Alpine Research* **2**: 303–312.

Haeberli W, Hallet B, Arenson L, Elconin R, Humlun O, Kaab A, Kaufmann V, Ladanyi B, Matsuoka N, Springman S, Vonder Muhll D. 2006. Permafrost creep and rock glacier dynamics. *Permafrost and Periglacial Processes* **17**: 189–214.

Harbor J, Wheeler DA. 1992. On the mathematical description of glaciated valley cross section. *Earth Surface Processes and Landforms* **17**: 477–485.

Harbor J, Warburton J. 1993. Relative rates of glacial and nonglacial erosion in alpine environments. *Arctic and Alpine Research* **25**: 1–7.

Harris C. 2005. Climate change, mountain permafrost degradation and geotechnical hazard. In *Global Change and Mountain Regions: An Overview of Current Knowledge*, Huber U, Bugmann H, Reasoner M (eds). Springer: Dordrecht; 215–225.

Hausmann H, Krainer K, Brückl E, Mostler W. 2007. Internal structure and ice content of the Reichenkar rock glacier (Stubai Alps, Austria) assessed by geophyiscal investigations. *Permafrost and Periglacial Processes* **18**: 351–367.

Hinderer M. 2001. Late Quaternary denudation of the Alps, valley and lake fillings and modern river loads. *Geodinamica Acta* **14**: 231–263.

Hoffmann T, Schrott L. 2002. Modelling sediment thickness and rockwall retreat in an Alpine valley using 2D-seismic refraction (Reintal, Bavarian Alps). *Zeitschrift für Geomorphologie, Supplement Band* **127**: 153–173.

Höllermann P. 1983. *Blockgletscher als Mesoformen der Periglazialstufe*. Bonner Geographische Abhandlungen: Bonn; 67.

Hufschmidt G. 2002. *GIS-gestützte Modellierung von Sedimentspeichern als Komponenten eines alpinen Geosystems (Reintal, Bayrische Alpen)*, Unpublished Diploma Thesis, University of Bonn.

Humlum O. 2000. The geomorphic significance of rock glaciers: estimates of rock glacier debris volumes and headwall recession rates in West Greenland. *Geomorphology* **35**: 41–67.

Jaboyedoff M, Baillifard F, Couture R, Locat J, Locat P. 2004. Towards preliminary hazard assessment using DEM topographic analysis and simple mechanic modeling. In *Landslide Evaluation and Stabilization*, Lacerda WA, Erhlich M, Fontoura AB, Sayo A (eds). Balkema: Amsterdam; 191–197.

Jaboyedoff M, Derron MH. 2005. A new method to estimate the infilling of alluvial sediment of glacial valleys using a sloping local base level. *Geografia Fisica e Dinamica Quaternaria* **28**: 37–46.

Jäckli H. 1957. *Gegenwartsgeologie des bündnerischen Rheingebiets. Ein Beitrag zur exogenen Dynamik alpiner Gebirgslandschaften*, Geotechnische Serie 36. Kümmerle & Frey: Bern.

Jordan P, Slaymaker O. 1991. Holocene sediment production in Lillooet river basin, British Columbia: a sediment budget approach. *Géographie Physique et Quaternaire* **45**: 45–57.

Kaab A, Reichmuth T 2005. Advance mechanisms of rock glaciers. *Permafrost and Periglacial Processes* **16**: 187–193.

Kääb A, Reynolds JM. 2005. Glacier and permafrost hazards in high mountains. In *Global Change and Mountain Regions: An Overview of Current Knowledge*, Huber U, Bugmann H, Reasoner M (eds). Springer: Dordrecht; 225–235.

Kelly MA, Buoncristiani JF, Schlüchter C. 2004. A reconstruction of the last glacial maximum (LGM) ice-surface geometry in the western Swiss Alps and contiguous Alpine regions in Italy and France. *Eclogae Geologicae Helvetiae* **97**: 57–75.

Li Y, Liu G, Cui Z. 2001. Glacial valley cross-profile morphology, Tian Shan Mountains, China. *Geomorphology* **38**: 153–166.

Molnar P, England P. 1990. Late Cenozoic uplift of mountain ranges and global climate change: chicken or egg? *Nature* **364**: 29–34.

Müller BU. 1999. Paraglacial sedimentation and denudation processes in an Alpine valley of Switzerland. An approach to the quantification of sediment budgets. *Geodinamica Acta* **12**: 291–301.

Nyenhuis M. 2006. *Permafrost und Sedimenthaushalt in einem alpinen Geosystem*, Bonner Geographische Abhandlungen 116. Department of Geography: Bonn.

Otto J-C, Dikau R. 2004. Geomorphic system analysis of a high mountain valley in the Swiss Alps. *Zeitschrift für Geomorphologie N.F.* **48**: 323–341.

Otto JC. 2006. *Paraglacial Sediment Storage Quantification in the Turtmann Valley, Swiss Alps*, PhD Thesis, University of Bonn.

Otto JC, Sass O. 2006. Comparing geophysical methods for talus slope investigations in the Turtmann valley (Swiss Alps). *Geomorphology* **76**: 257–272.

Otto JC, Kleinod K, Konig O, Krautblatter M, Nyenhuis M, Roer I, Schneider M, Schreiner B, Dikau R. 2007. HRSC-A data: a new high-resolution data set with multipurpose applications in physical geography. *Progress in Physical Geography* **31**: 179–197.

Owen LA, England J. 1998. Observations on rock glaciers in the Himalayas and Karakoram Mountains of northern Pakistan and India. *Geomorphology* **26**: 199–213.

Owens PN, Slaymaker O. 1992. Late Holocene sediment yield in small alpine and subalpine drainage basins, British Columbia. *Proceedings of the Chengdu Symposium: Erosion, Debris Flows and Environments in Mountain Regions*, July; 147–154.

Pfiffner OA, Heitzmann P, Lehner P, Frei W, Pugin P, Felber M. 1997. Incision and backfilling of the Alpine valleys: Pliocene and Holocene processes. In *Deep Structure of the Swiss Alps. Results of NRP 20*, Pfiffner OA, Lehner P, Heitzmann P, Mueller S, Steck A (eds). Birkhäuser: Basel; 265–288.

Rapp A. 1960. Recent development of mountain slopes in Kaerkevagge and surroundings, Northern Scandinavia. *Geografiska Annaler A* **42**: 1–200.

Rosselli A, Olivier R. 2003. Modélisation gravimétrique 2.5D et cartes des isohypses au 1:100,000 du substratum de la vallée du Rhone entre Villeneuve et Brig (Suiss). *Eclogae Geologicae Helvetiae* **96**: 399–423.

Sass O. 2007. Bedrock detection and talus thickness assessment in the European Alps using geophysical methods. *Journal of Applied Geophysics* **62**: 254–269.

Sass O. 2006. Determination of the internal structure of alpine talus deposits using different geophysical methods (Lechtaler Alps, Austria). *Geomorphology*. **80**: 45–58.

Sass O, Wollny K. 2001. Investigations regarding alpine talus slopes using ground-penetration radar (GPR) in the Bavarian Alps, Germany. *Earth Surface Processes and Landforms* **26**: 1071–1086.

Schlunegger F, Hinderer M. 2001. Crustal uplift in the Alps: why the drainage pattern matters. *Terra Nova* **13**: 425–432.

Schlunegger F, Hinderer M. 2003. Pleistocene/Holocene climate change, re-establishment of fluvial drainage network and increase in relief in the Swiss Alps. *Terra Nova* **15**: 88–95.

Schrott L, Adams T. 2002. Quantifying sediment storage and Holocene denudation in an Alpine basin, Dolomites, Italy. *Zeitschrift für Geomorphologie N.F. Supplement Band* **128**: 129–145.

Schrott L, Niederheide A, Hankammer M, Hufschmidt G, Dikau R. 2002. Sediment storage in a mountain catchment: geomorphic coupling and temporal variability (Reintal, Bavarian Alps, Germany). *Zeitschrift für Geomorphologie* **127**: 175–196.

Schrott L, Hufschmidt G, Hankammer M, Hoffmann T, Dikau R. 2003. Spatial distribution of sediment storage types and quantification of valley fill deposits in an alpine basin, Reintal, Bavarian Alps, Germany. *Geomorphology* **55**: 45–63.

Schrott L, Sass O. 2008. Application of field geophysics in geomorphology: advances and limitations exemplified by case studies. *Geomorphology* **93**: 55–73.

Shroder JF, Scheppy RA, Bishop MP. 1999. Denudation of small alpine basins, Nanga Parbat Himalaya, Pakistan. *Arctic Antarctic and Alpine Research* **31**: 121–127.

Slaymaker O, Spencer T. 1998. *Physical Geography and Global Environmental Change. Understanding Global Environmental Change. 1*. Addison Wesley Longman Limited: Harlow.

Small RJ. 1987. Moraine sediment budgets. In *Glacio-fluvial Sediment Transfer – An Alpine Perspective*, Gurnell AM, Clark MJ (eds). John Wiley & Sons: Chichester; 165–198.

Taylor SB, Kite JS. 2006. Comparative geomorphic analysis of surficial deposits at three central Appalachian watersheds: implications for controls on sediment-transport efficiency. *Geomorphology* **78**: 22–43.

Watanabe T, Dali L, Shiraiwa T. 1998. Slope denudation and the supply of debris to cones in Langtang Himal, Central Nepal Himalaya. *Geomorphology* **26**: 185–197.

Wheeler DA. 1984. Using parabolas to describe the cross-sections of glaciated valleys. *Earth Surface Processes* **9**: 391–394.

Zimmermann M, Haeberli W. 1992. Climatic change and debris flow activity in high-mountain areas – a case study in the Swiss Alps. *Catena Supplement* **22**: 59–72.